CHRONIC FLUORIDE EXPOSURE DISRUPTS BRAIN EXTRACELLULAR MATRIX AND INDUCES NEUROTOXICITY IN RATS

A. Dahiru[1,2], Z. Fatima[1], I. Nawaz[1], S. K. Riaz[3*], M. Abbas[1], M. N. Shafqat[1], M. J. Khan[1], A. Q. Khan[4], S. A. M A. S. Eqani[1*]

[1]Department of Biosciences, COMSATS University Islamabad, Islamabad, Pakistan.
[2]Department of Veterinary Physiology and Biochemistry, Usmanu Danfodiyo University, Sokoto, Nigeria.
[3]Department of Molecular Biology, Shaheed Zulfiqar Ali Bhutto Medical University, Islamabad, Pakistan
[4]Department of Pathology, Pakistan Institute of Medical Sciences, Islamabad, Pakistan
*Corresponding Author's email: alishah@comsats.edu.pk

ABSTRACT

Fluoride is widely distributed in the environment, and excessive exposure has been associated with adverse effects in humans and animals. However, its effects on extracellular matrix (ECM) remodeling and collagen-related molecular pathways in the brain remain inadequately characterized. This study investigated the effects of different doses of sodium fluoride on the expression of ECM and collagen-related genes, and histopathological alterations in rat brain tissues. The findings are expected to provide baseline evidence for understanding ECM and collagen-associated alterations in fluoride-induced neurotoxicity. Using complete randomized design, forty Sprague-Dawley rats (20 males and 20 females) were allocated to four groups (n = 10/group; 5 males and 5 females) and exposed to 0.5 ppm (control), 50, 150, and 300 ppm NaF in drinking water for 90 days. Masson's trichrome staining of brain tissues was performed to assess collagen deposition and tissue remodeling, while the expressions of *COL1A1*, *COL1A2*, and *MMP9* were quantified using RT-qPCR. Masson's trichrome staining revealed collagen deposition and extracellular matrix remodeling, accompanied by structural alterations, particularly in brain tissues exposed to higher NaF doses. Chronic NaF exposure was associated with dose-dependent downregulation ($p \leq 0.05$) of *COL1A1* expression (0.69-, and 0.47-fold at 150, and 300 ppm, respectively), compared with the control. *COL1A2* expression was also downregulated, particularly in male rats ($p \leq 0.05$), with expression levels of 0.39-, 0.85-, and 0.57-fold, respectively. *MMP9* expression showed a decreasing trend ($p > 0.05$) with increasing NaF exposure in both sexes. These findings suggest that chronic NaF exposure is associated with alterations in brain ECM-related gene expression and tissue architecture. The observed changes provide baseline evidence for further investigation of ECM remodeling and its potential involvement in fluoride-induced neurotoxicity.

Keywords: Fluoride, Extracellular matrix remodeling, Collagen, Neurotoxicity, *COL1A1*, *COL1A2*, *MMP9*

This article is an open access article distributed under the terms and conditions of the Creative Commons Attribution (CC BY) license (https://creativecommons.org/licenses/by/4.0

https://doi.org/10.36899/JAPS.2026.6.0152 Published first online October 10, 2026

INTRODUCTION

Fluoride is naturally present in food, plants, and drinking water at varying levels in the environment (Kashyap *et al*., 2021) and is considered one of the most important elements involved in dental and skeletal mineralization (Johnston and Strobel, 2020). Fluoride is crucial for the skeletal system's growth, development, and maintenance at low concentrations, while at high concentrations it can harm various tissues and organs, particularly the teeth and skeleton, leading to fluorosis (Bibi *et al*., 2023; Dahiru *et al*., 2026; Yan *et al*., 2011). Fluorosis is a chronic systemic disease that affects individuals living in fluoride-contaminated areas due to long-term excessive fluoride ingestion via drinking water (Bibi *et al*., 2023; Ren *et al*., 2022; Sadiq *et al*., 2025). Contaminated groundwater is the primary source of fluoride exposure at the regional scale, and around 783 million people are dependent on fluoride contaminated drinking water (Lacson *et al*., 2021). Fluoride exposure greater than the WHO guideline value (1.5 mg/L) can cause dental and skeletal fluorosis, whereas lower fluoride concentrations in potable drinking water (≤0.5 mg/L) are recognized to reduce tooth decay (Jagtap *et al.*, 2012). Previous studies have also reported that fluoride can cross the blood-brain barrier and accumulate in brain tissue, thereby being linked with neurotoxic effects, even at drinking water fluoride concentrations as low as 1 ppm (Varner *et al*., 1998). These toxic effects of fluoride exposure include alterations in the integrity of neuronal and cerebrovascular membranes (Varner *et al.*, 1998) and abnormal behavior patterns (Mullenix *et al*., 1995).

Extracellular matrix (ECM) is a network of macromolecules composed of enzymes, collagen, and proteins that provide biochemical and structural support to the tissues (Laronha and Caldeira, 2020). The components that make up the

extracellular matrix include fibers (collagen, laminin, elastin, and fibronectin), proteoglycans (aggrecan and syndecan-1), glycoproteins (entactin, tenascin and vitronectin), and polysaccharides (hyaluronic acid) (Liu and Khalil, 2017). The ECM function includes the regulation of cell migration, proliferation, and differentiation (Zhu *et al.,* 2018). The various factors that affect the turnover and new synthesis of particular ECM components ultimately dictate the ECM's composition (Rutnam *et al*., 2013).

Collagen is the most abundant protein in ECM that provides cells with structural support (Cui *et al*., 2017). The collagen family comprises a diverse group of proteins that are major component of the extracellular matrix, particularly in bones, cartilage and other connective tissues where they are attributed to tissue strength, flexibility and structural integrity. The human genome contains approximately thirty different collagen genes, which are transcribed and translated into proteins that combine in various ways to produce about 20 different types of collagen fibrils (Cui *et al*., 2017). Numerous cell types produce collagen molecules, and there are many instances in which collagen regulates cell phenotypes (Rutnam *et al*., 2013). Collagen is a major structural component of the extracellular matrix in brain, collagen types I and IV are particularly important elements of the connective tissues and basal lamina, respectively (Myllyharju and Kivirikko, 2004). Type I collagen is a heterotrimer composed of two alpha 1(I) and one alpha 2(I) polypeptide chains, corresponding to an approximate 2:1 chain stoichiometry ratio. These chains are encoded by *COL1A1* and *COL1A2*, respectively (Sharma *et al.,* 2017). According to previous research, defects in collagen production may contribute to fluoride-induced hard-tissue lesions, as collagen is the main structural element of teeth and bones.

Matrix metalloproteinases (MMPs) are a class of proteolytic enzymes that share common structural characteristics but differ in their substrate specificities. These zinc-dependent endopeptidases play important roles in numerous biological processes, including cell migration, differentiation, adhesion, and extracellular matrix remodeling (Laronha and Caldeira, 2020). The MMP family in human comprises 25 members characterized by a conserved catalytic domain containing zinc-binding motif (HEXGHXXGXXH), an apo-domain (Chambers and Matrisian, 1997), along with other structurally conserved domains (Laronha and Caldeira, 2020). Depending on their substrate specificity, domain organization and structural/functional characteristics, MMPs are commonly classified into several subgroups, including collagenases, gelatinases, stromelysins and membrane-type matrix metalloproteinases are the four subgroups of the MMP family (Malemud, 2006).

Despite growing evidence of fluoride-induced toxicity, the effects of fluoride exposure on extracellular matrix (ECM) remodeling in brain, particularly on the expression of collagen-related genes and matrix metalloproteinases, remain poorly understood. In addition, the relationship between these molecular alterations and histopathological changes associated with fluoride-induced neurotoxicity has not been sufficiently investigated. Therefore, the present study was designed to evaluate the effects of chronic fluoride exposure on the expression of selected ECM-related genes, including *Collagen Type I Alpha 1 Chain* (*COL1A1*), *Collagen Type I Alpha 2 Chain* (*COL1A2*), and *Matrix Metalloproteinase 9* (*MMP9*), and to assess associated histopathological alterations in the brain tissues of rats. By examining both molecular and histopathological endpoints, this study aims to provide baseline data for further investigation of potential involvement of ECM remodeling in fluoride-induced neurotoxicity.

MATERIALS AND METHODS

Materials: The following reagents and instruments were used in this study: sodium fluoride (NaF; analytical grade; Sigma-Aldrich, St. Louis, MO, USA), TRIzol® reagent (Cat. No. 15596-018, Invitrogen, USA), DNA ladder (Cat. No. 15628019, Invitrogen, USA), RevertAid First-Strand cDNA Synthesis Kit (Cat. No. K1622, Thermo Fisher Scientific, USA), SYBR Green Master Mix (Thermo Fosher Scientific, USA), DreamTaq Green PCR Master Mix (Thermo Fisher Scientific, USA). RNA concentration and purity were determined using a NanoDrop spectrophotometer (IMPLEN N60, Germany), and Real-Time quantitative PCR (RT-qPCR) was performed using a QuantStudio 5 Real-Time PCR System (Thermo Fisher Scientific, USA).

Experimental Animals: Ethical approval for the study was granted by the National Institutes of Health (NIH), Pakistan (Approval No. F-1/EAC/2024). The study was conducted in accordance with the guidelines for the care and use of laboratory animals described by Albus, (2012). Forty Sprague-Dawley rats (20 males and 20 females), aged 5 weeks at the beginning of the experiment, were procured from the NIH animal facility. The baseline body weights ranged from 186 to 209 g in males and from 140 to 180 g in females. The rats were housed in well-ventilated cages and provided with a standard rodent diet with tap water *ad' libitum*. The animals were acclimatized for one week before the start of the experiment (Tonetto *et al*., 2023) and maintained at a room temperature of 25 ± 4°C and relative humidity of 40 - 60% under a 12-hours light/12-hours dark cycle.

Study Design: The study was conducted using a complete randomized design (CRD), with a 2 x 4 factorial arrangement, comprising two sex and four NaF treatment levels. Forty rats were randomly assigned to four experimental groups (n =

10/group; 5 males and 5 females) viz; control, low-dose, medium-dose, and high-dose groups, with the aim of maintaining balanced sex distribution and comparable baseline body weights among the treatment groups. The low-, medium- and high-dose groups received drinking water containing 50, 150 and 300 ppm NaF, respectively. The selected NaF concentrations were based on previous toxicological studies (Heindel *et al*., 1996). Based on an assumed water consumption of 150 mL/kg body weight/day, these concentrations corresponded to estimated daily NaF intakes of 7.5, 22.5, and 45 mg/kg/day, respectively. Because individual water consumption was not measured, these values represent estimated rather than directly measured NaF intakes, and actual exposure may have varied among individual animals, treatment groups, and sexes. The control group received drinking water containing 0.5 ppm NaF. This concentration was selected as the control condition to provide a low background level of fluoride while minimizing the likelihood of fluoride-related toxic effects. Animals were continuously exposed to their respective drinking-water treatments for 90 consecutive days.

Brain Tissues Collection: At the end of the 90-day exposure period, rats were euthanized using approved anesthetic protocol, and the brain was carefully removed after opening the skull. A sagittal section was made through the brain, and the cerebral cortex and hippocampus were carefully dissected. Tissue samples designated for molecular analysis were immediately placed in RNAlater (Aboghazleh *et al*., 2024) and stored at -40 ^{o}C until RNA extraction. Separate portions of the brain tissue were collected and fixed in 10% neutral buffered formalin for subsequent histopathological evaluation.

Histopathological Analysis: Brain tissues were collected and fixed using (10%) buffered formalin for histopathological investigation. Following fixation and routine tissue processing, sections were prepared and stained with Masson's trichrome to assess collagen deposition and extracellular matrix (ECM) alterations in the hippocampus and cerebral cortex of male and female rats. Based on our previous findings, which demonstrated fluoride-induced morphological alterations in brain tissue, including cellular shrinkage, pyknosis, extracellular oedema, and vacuolization (Dahiru *et al*., 2026), Masson's trichrome staining was additionally performed in the present study to further investigate collagen deposition and ECM alterations. Two histopathologists, blinded to treatment groups, independently evaluated the sections to minimize observer bias. In the present study, six histopathological features associated with collagen deposition and tissue integrity, , including the extent of collagen staining, collagen fiber thickness, and pattern, perivascular inflammation, tissue integrity, and fibrosis, were assessed semi-quantitatively, using a four-point ordinal scoring scale (0 = absent, 1 = mild, 2 = moderate, and 3 = severe). For each animal, 10 randomly selected, non-overlapping fields from each examined brain region were evaluated at 40x magnification using a light microscope (Olympus CX-23, Evident, Tokyo, Japan). The animal was considered the experimental unit, and the observations from the examined fields were used to characterize the severity of histopathological changes for each animal and to compare the experimental groups.

Total RNA Extraction: Brain tissue (100 mg) was used for total RNA extraction using TRIzol® reagents according to the manufacturer's instructions. The concentration of the extracted RNA was determined using a Nanodrop spectrophotometer, and RNA purity was assessed by measuring the A260/A280 absorbance ratio (ranged between 1.8 - 2.0). RNA integrity was further evaluated by native agarose gel electrophoresis.

cDNA Synthesis: The extracted RNA was used to synthesize complementary DNA (cDNA) in a 20 µL reaction volume using RevertAid First-Strand cDNA synthesis kit according to manufacturer's instructions. For each reaction, total RNA (1000 ng), was used for cDNA synthesis. The synthesized cDNA was stored at -20°C until further use.

Primers Design: The primers for *Collagen Type I Alpha I Chain* (*COL1A1*), *Collagen Type I Alpha 2 Chain* (*COL1A2*), *Matrix Metalloproteinase* (*MMP9*) and the reference gene *glyceraldehyde-3-phosphate dehydrogenase* (*GAPDH*) were designed (Table 1) using the PrimerQuest Tool (Integrated DNA Technology, IA, USA) (https://www.idtdna.com/PrimerQuest/Home/Index) and validated using NCBI primer-BLAST(https://www.ncbi.nlm.nih.gov/tools/primer-blast/). The primer sequences and relevant primer details are mentioned in Table 1. The corresponding reference sequences were obtained from the NCBI GenBank database using the following accession numbers; NM_053304.1 for *COL1A1*, NM_053356.2 for *COL1A2* NM_031055.2 for *MMP9* and NM_017008.4 for *GAPDH*. To eliminate the potential amplification from genomic DNA, the primers were designed to flank an intron by targeting the exon-exon junctions.

Genes Expression: The RT-qPCR was performed in a final reaction volume of 10 µL. Each reaction contained 1 µL of 10-fold diluted cDNA, 2 µL of primer mixture (sense and antisense-10 times diluted), 2 µL of nuclease-free water, and 5 µL of SYBR Green Master Mix. *GAPDH* was used as the internal reference gene for normalization of target gene expression. Each sample was analyzed in technical duplicate, and the mean cycle threshold (Ct) value was used for subsequent analysis. Relative fold expression was calculated using the $2^{\wedge-\Delta\Delta Ct}$ method. The thermal cycling conditions for RT-qPCR, were as follows: initial denaturation at 94 ^{o}C for 3 min, followed by 35 cycles of denaturation at 94 ^{o}C for 30 sec, annealing at 58 ^{o}C for 30 sec, and extension at 72 ^{o}C for 45 sec, followed by a final extension at 72 ^{o}C for 10 min. The

same cycling conditions were applied to all target and reference gene reactions. Following amplification, the RT-qPCR products were electrophoresed on 2% agarose gels, stained with ethidium bromide, and visualized under UV-light gel viewer to verify the expected amplicon size.

Table 1: List of primers sequences and amplicons sizes used for RT-qPCR.

Gene	Sense Primer (5′ to 3′)	Antisense Primer (5′ to 3′)	Annealing Temp (ºC)	Amplicons length (bp)
COL1A1	GAGCCAGCAGATTGAGAAC	TTAGGGTCGATCCAGTACTCTC	60	124
COL1A2	CAGACCCAAGGACTATGAAG	GGTTAGGGTCAATCCAGTAG	60	167
MMP9	GATCCGCAGTCCAAGAAGAT	CTGAGCCTAGACCCAACTTATC	58	109
GAPDH	GATGCTGGTGCTGAGTATGT	GCGGAGATGATGACCCTTT	58	104

Key: *COL1A1* (*Collagen Type I Alpha I Chain*), *COL1A2* (*Collagen Type I Alpha 2 Chain*), *MMP9* (*Matrix Metalloproteinase*) and *GAPDH* (*Glyceraldehyde-3-phosphate dehydrogenase*).

Statistical Analysis: The data were analyzed using SPSS (Version 22) and GraphPad Prism 5 (GraphPad Software, Inc., CA, USA). Quantitative data were summarized using descriptive statistics and presented as mean ± standard deviation (SD). The assumption of homogeneity of variance was assessed using Levene's test. The assumption was satisfied for baseline body weight in males ($p = 0.555$), females ($p = 0.383$), and both sexes combined ($p = 0.314$). Two-way analysis of variance (ANOVA) was performed to evaluate the main effects of NaF treatment (control-, low-, medium-, and high-dose), sex (male and female), and the NaF treatment*sex interaction on the quantitative outcomes, followed by Tukey's *post hoc* test for multiple comparisons. Repeated measure ANOVA was used to assess changes in body weight over time and to evaluate difference in body weight trajectories among experimental groups. Correlation analysis was performed to assess the associations among the expression levels of the three target genes. Categorical histopathological findings were analyzed using the chi-square test to assess differences in the distribution of lesions among experimental groups. A p value ≤ 0.05 was considered statistically significant.

RESULTS

Effect of sodium fluoride (NaF) exposure on rat body weight: All rats in the control and treatment groups showed a progressive increase in body weight over the exposure period ($p \leq 0.001$), with this pattern observed in both males and females. However, there was no significant effect of NaF treatment on body weight ($p = 0.05$) and the dose*sex interaction (**Figure** 1 A & B).

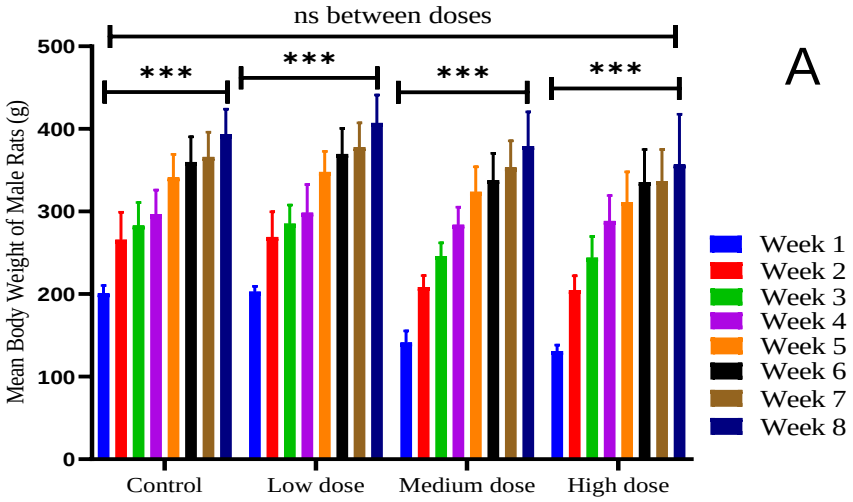

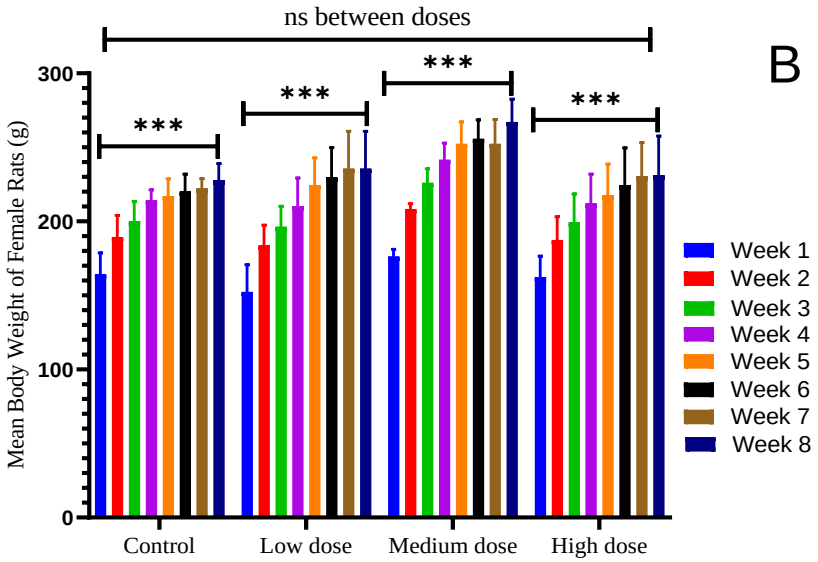

Figure 1: Mean ± SD of body weight of (A) male and (B) female rats. Rats were exposed to control (0.5 ppm), low (50 ppm), medium (150 ppm), and high (300 ppm) NaF concentrations. Asterisk's (***) indicate statistically significant difference, whereas "ns" indicates a non-significant difference.

Histopathological alterations in the brain tissue of fluoride-exposed rats: Masson's trichrome staining was performed to evaluate collagen deposition and extracellular matrix (ECM) alterations in the hippocampus and cerebral cortex of male (**Figure** 2) and female (**Figure** 3) rats following 90 days of NaF exposure.

The control group showed normal histoarchitecture, with intact neuronal morphology and no appreciable collagen deposition in either the hippocampus or cerebral cortex (**Figure** 2-3). The low dose group (50 ppm) similarly showed no appreciable collagen deposition, although slight perivascular changes were observed. In the medium dose group (150 ppm), mild collagen accumulation was observed, accompanied by increased extracellular oedema and mild neuronal degeneration. In the high dose group (300 ppm), more pronounced fluoride-induced collagen deposition was observed, characterized by discrete, blue-stained perivascular and interstitial collagen fibers, accompanied by marked disruption of normal tissue architecture, including neuronal shrinkage, pyknosis, vacuolization and degenerative changes (Dahiru *et al.*, 2026) (**Figure** 2-3).

Chi-square tests of independence were conducted to examine the altered histopathological features by Masson's trichrome staining among the experimental groups following fluoride exposure. Statistically significant associations were observed for the extent of collagen staining (χ^2 = 10.59, df = 3, $p \leq 0.05$), collagen fiber thickness (χ^2 = 10.59, df = 3, $p \leq 0.05$), collagen fiber pattern (χ^2 = 15.00, df = 3, $p \leq 0.05$), perivascular inflammation (χ^2 = 14.73, df = 3, $p \leq 0.05$), tissue integrity (χ^2 = 14.73, df = 3, $p \leq 0.05$), and fibrosis (χ^2 = 10.59, df = 3, $p \leq 0.05$) (**Figure** 4).

The severity distribution of degenerative lesions differed significantly ($p \leq 0.05$) among exposure groups in male rats whereas the difference did not reach statistical significance in female rats. These finding suggest that histopathological alterations were more pronounced in male rats than in female rats. Regionally, histopathological alterations were more evident in the hippocampus than in the cerebral cortex, indicating greater regional susceptibility to fluoride-induced neurotoxicity. Overall, the distribution of lesion severity differed significantly among exposure groups for neuronal degeneration, extracellular oedema and vacuolization. Taken together, the histopathological findings showed greater changes with increasing NaF exposure, with more pronounced changes observed in male rats than in female rats.

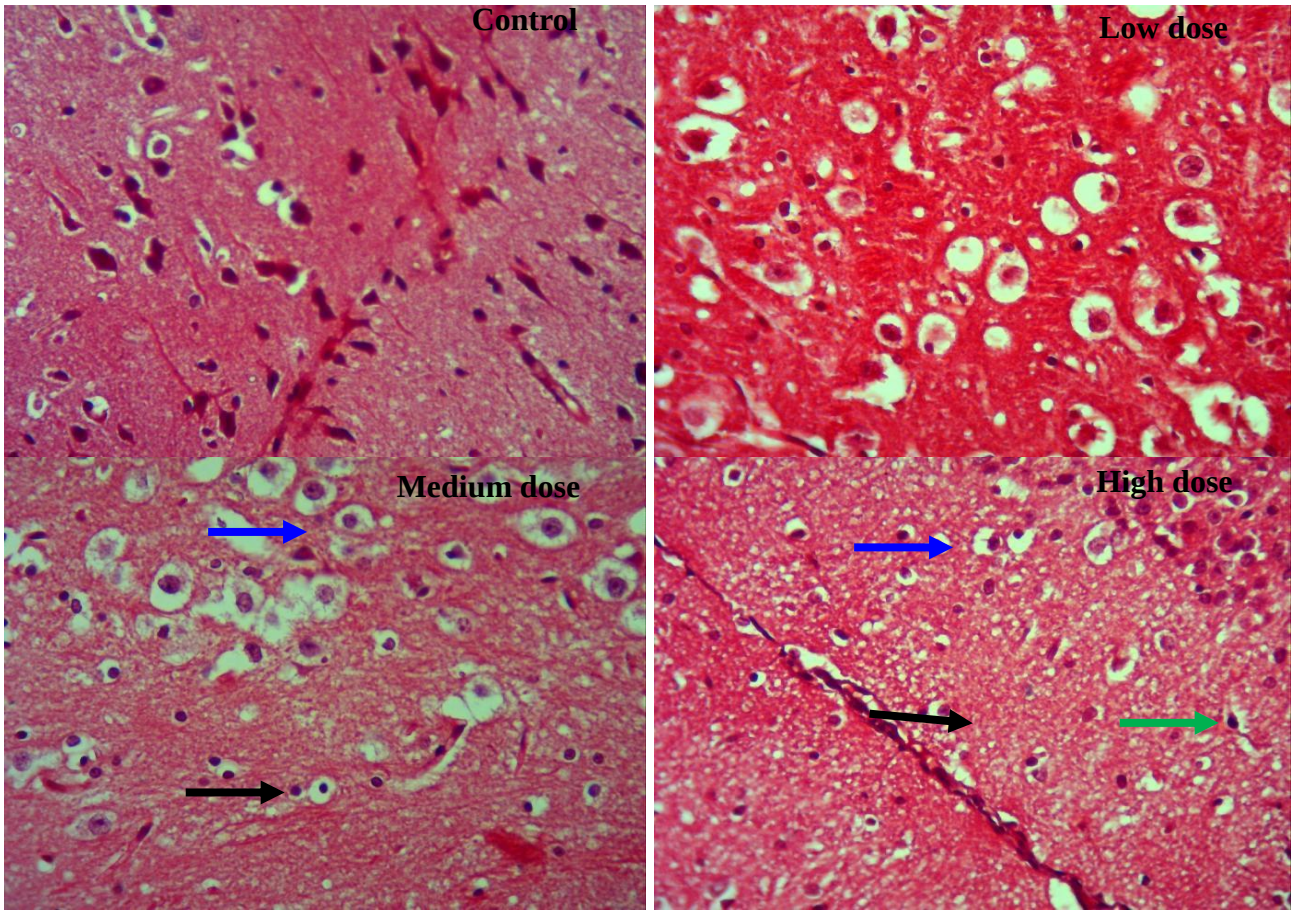

Figure 2: Masson's trichrome-stained sections of the hippocampus and cerebral cortex of male rats from the control and sodium fluoride (NaF)-exposed groups following 90 days of exposure. Collagen fibers are stained blue, whereas muscle and cytoplasm appear red and nuclei are stained dark. The medium-dose group (150 ppm) showed increased extracellular edema (black arrow) and mild neuronal degeneration (blue arrow) (Dahiru et al., 2026), whereas the high-dose group (300 ppm) showed collagen deposition (green arrow),neuronal degeneration, including neuronal shrinkage (black arrow), and pyknosis and vacuolization (blue arrow) (Dahiru *et al*., 2026). Images were captured at 40x magnification.

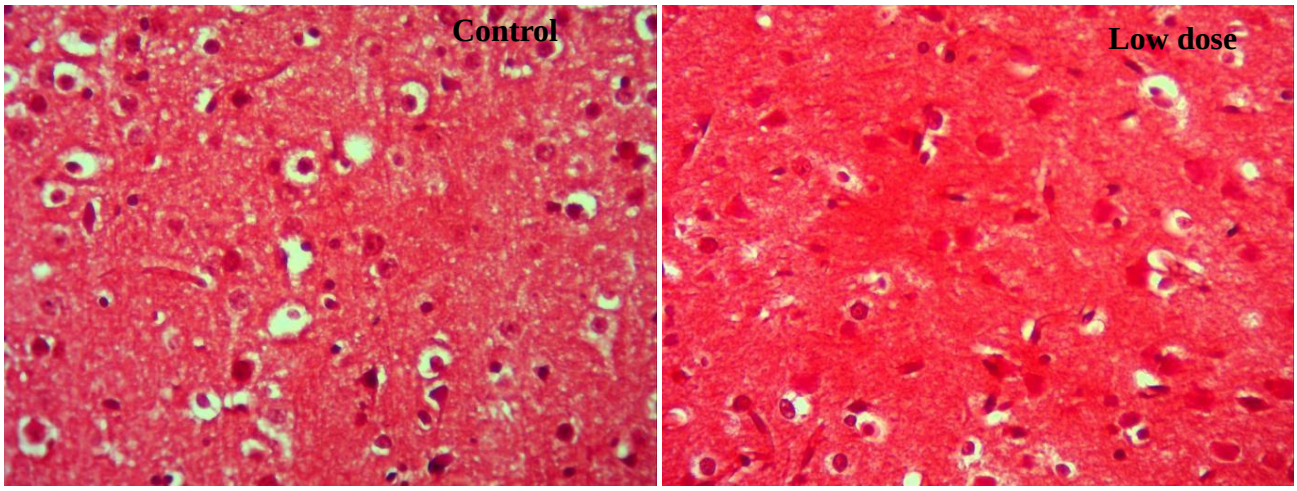

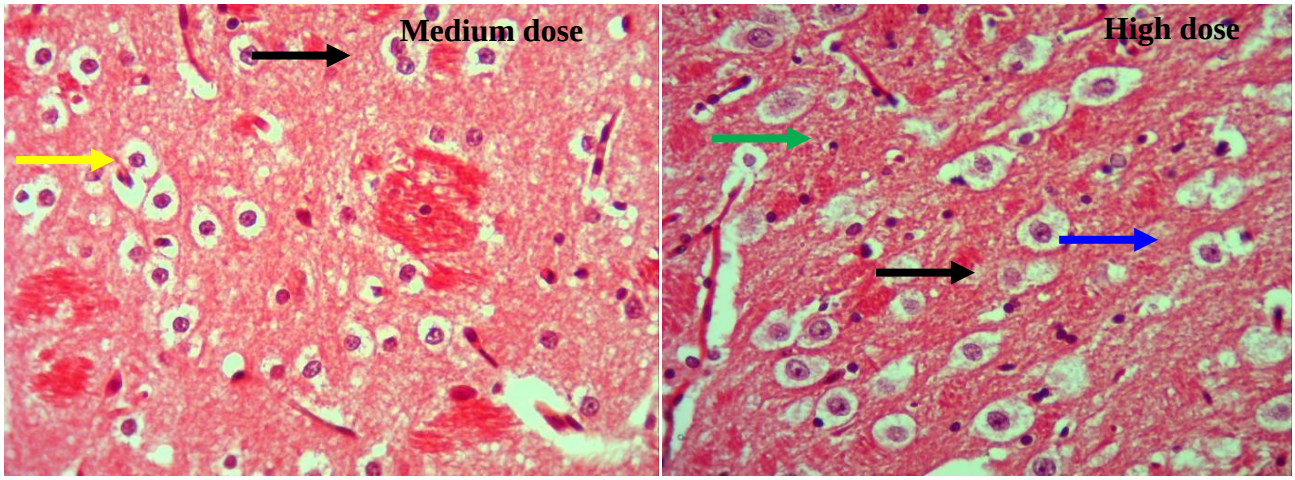

Figure 3: Masson's trichrome-stained sections of the hippocampus and cerebral cortex of female rats from the control and sodium fluoride (NaF)-exposed groups following 90 days of exposure. Collagen fibers are stained blue, whereas muscle and cytoplasm appear red and nuclei are stained dark. The medium-dose group (150 ppm) showed no appreciable collagen accumulation but exhibited increased extracellular edema (yellow arrow) and neuronal degeneration (black arrow) (Dahiru et al., 2026). The high-dose group (300 ppm) showed fluoride-induced collagen deposition (green arrow), neuronal degeneration, including neuronal shrinkage (black arrow), and pyknosis and vacuolization (blue arrow) (Dahiru *et al.*, 2026). Images were captured at 40x magnification.

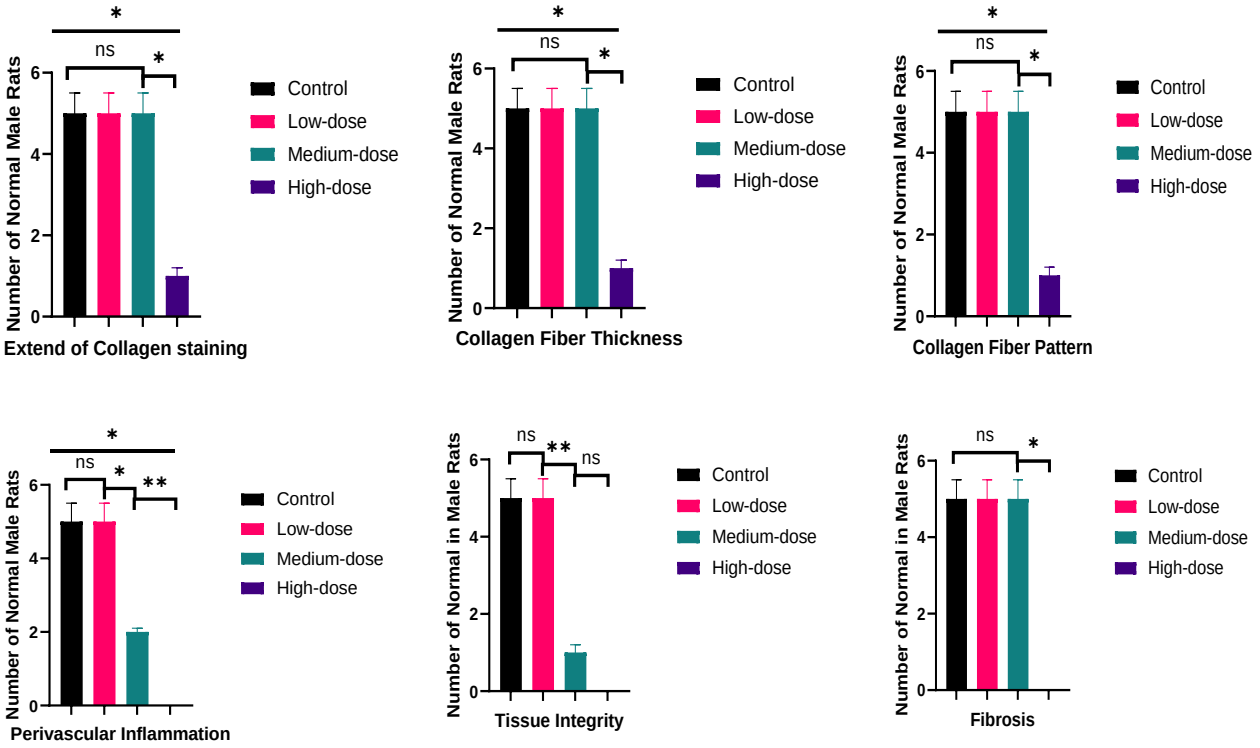

Figure 4: Distribution of male and female rats according to histopathological parameters assessed using Masson's trichrome staining following 90 days of NaF exposure. Bars represent the number of rats classified according to the observed severity of collagen staining (extent), collagen fiber thickness, collagen fiber pattern, perivascular inflammation, tissue integrity, and fibrosis. Statistical comparisons were performed using the chi-square test; $p \leq 0.05$, $p \leq 0.01$, and ns (not significant).

Effect of chronic fluoride exposure on *COL1A1, COL1A2* and *MMP9* expression: Chronic fluoride exposure produced a significant downregulation of *COL1A1*, *CL1A2* and *MMP9* transcripts level in the brain tissue of exposed rats compared to those of controls ($p \leq 0.05$). Two-way ANOVA revealed a significant main effect of dose for all three genes, whereas neither the main effect of sex nor the dose*sex interaction reached statistical significance. Tukey post hoc comparison confirmed significant reductions in the expression levels for medium- ($p \leq 0.05$) and high-dose ($p \leq 0.05$) groups relative to control, while the low-dose group did not differ significantly from control (**Figures** 5-7).

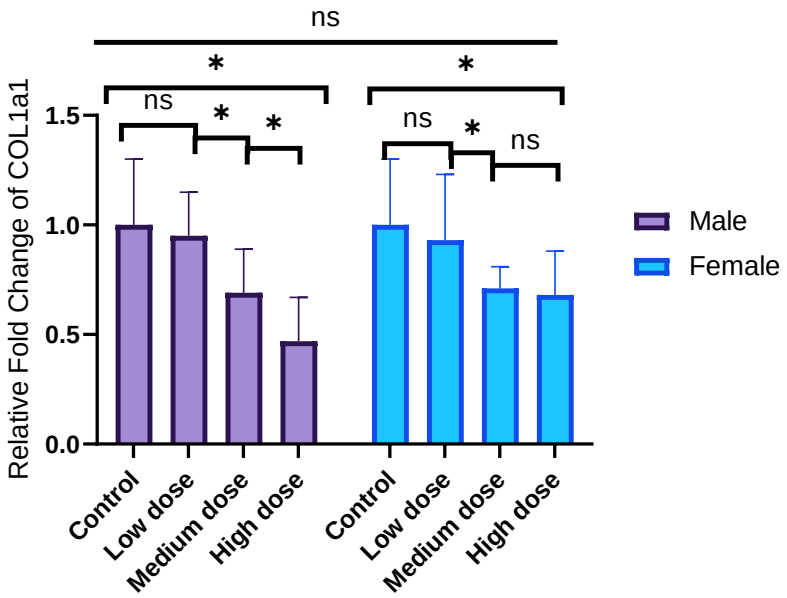

Figure 5: Relative fold expression of *COL1A1* (mean ± SD) in male and female rat's brain tissue (N = 5). Asterisks (*) indicate level of significance as *p≤0.05*, while ns (non-significant).

COL1A1 expression showed a dose-dependent downregulation in both male and female rats, with expression reduced to 0.69-fold at the medium dose and 0.47-fold at the high dose, relative to the controls ($p \leq 0.05$) (**Figure** 5). No significant effect of sex or dose*sex interaction was observed, indicating that the *COL1A1* response to fluoride exposure did not differ significantly between male and female rats. However, a significant difference ($p \leq 0.05$) between medium and high dose groups was observed in males in contrast to females.

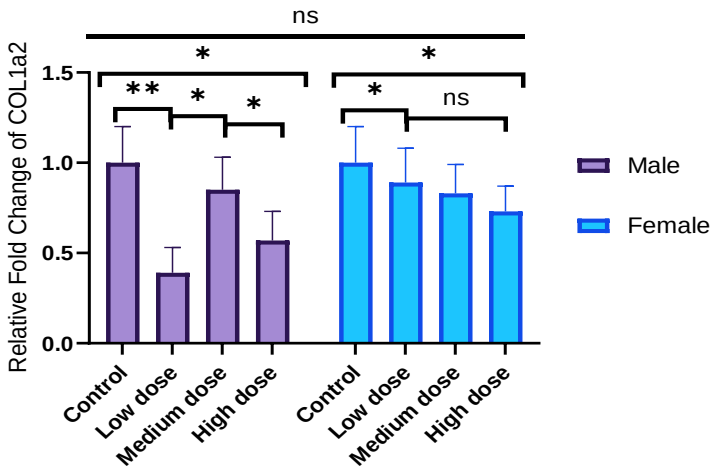

Figure 6: Relative fold expression of *COL1A2*, (mean ± SD) in male and female rat's brain tissue (n = 5). Asterisks (*) and (**) indicate level of significance as *p≤0.05* and *p≤0.001*, respectively while ns (non-significant).

For *COL1A2*, in male rats, expression was significantly downregulated at low, medium, and high fluoride doses, with expression levels of 0.39-fold (low dose), 0.85-fold (medium dose), and 0.57-fold (high dose), relative to the controls, respectively ($p \leq 0.05$). In females, *COL1A2* expression showed a progressive decline with increasing fluoride exposure, reaching 0.89-, 0.83-, and 0.73-fold of the transcript levels at low, medium, and high doses, respectively compared to the control (**Figure** 6). The overall effect of fluoride exposure was characterized by downregulation of *COL1A2* expression (**Figure** 6); however, the dose*sex interaction was not significant, indicating that the response did not differ significantly between male and female rats.

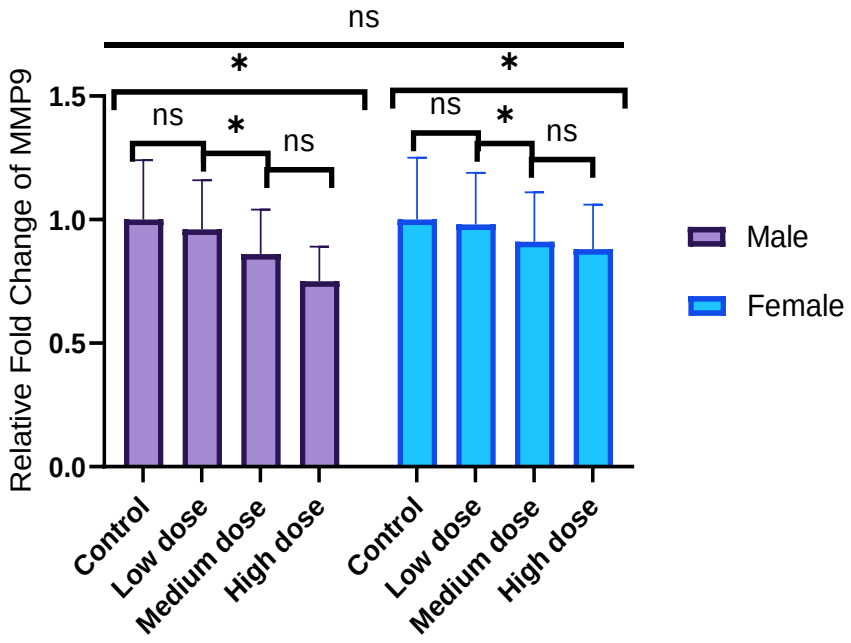

Figure 7: Relative fold expression of *MMP9* (mean ± SD) in male and female rat's brain tissue (n = 5). Asterisks (*) and (**) indicate level of significant as *P≤0.05*, while ns (non-significant).

MMP9 expression was downregulated following chronic fluoride exposure in both male and female rats (**Figure** 7). In male rats, medium and high dose of fluoride exposure reduced *MMP9* expression to 0.86-fold and 0.75-fold compared to the control, respectively, whereas in female rats, expression decreased to 0.98-fold, 0.91-fold, and 0.88-fold at low, medium, and high doses, respectively. The dose*sex interaction was not significant, indicating that the pattern of *MMP9* expression did not differ significantly between male and female rats (**Figure** 7).

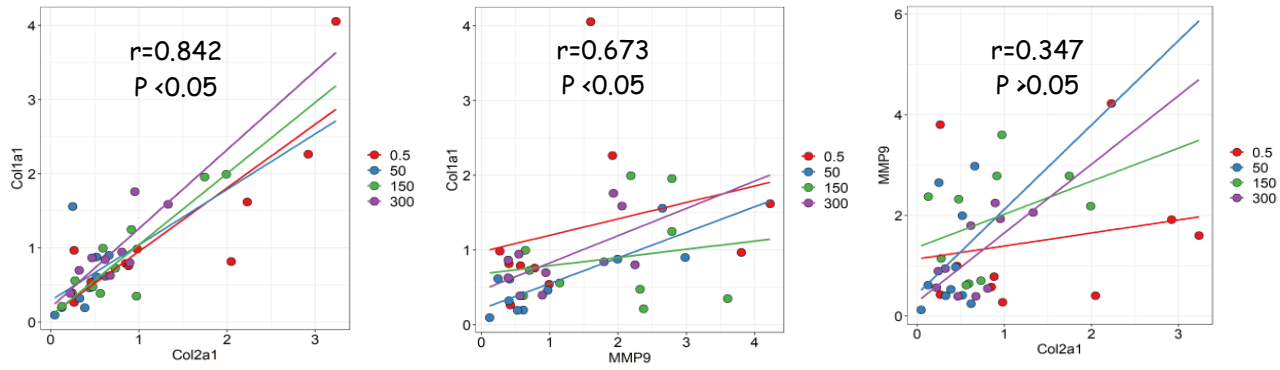

Figure 8: Scatter plots showing the associations between the relative expression levels of *COL1A1*, *COL1A2* and *MMP9*. Spearman's rank correlation analysis was performed to assess the strength and direction of the relationships among the investigated genes. Each point represents an individual animal, and the red line indicates the fitted regression trend line.

Spearman correlation analysis revealed strong positive correlation between *COL1A1* versus *COL1A2* (r = 0.842, $p \leq 0.05$), and positive association with *MMP9* (r = 0.673, $p \leq 0.05$). A weak positive correlation was observed between *COL1A2 and MMP9* (r = 0.347, $p > 0.05$) (**Figure** 8).

DISCUSSION

The present study revealed that chronic NaF exposure was associated with alterations in extracellular matrix (ECM) homeostasis in the brain, as evidenced by the downregulation of *COL1A1*, *COL1A2* and *MMP9* expression in brain tissue. Although fibrillar collagen is a relatively minor constituent of brain parenchyma compared with peripheral tissues, it contributes to the structural integrity and homeostasis of specialized ECM compartments within the central nervous system. In the CNS, collagen is predominantly associated with vascular and meningeal basement membranes, with type I collagen reported main in the meninges and perivascular spaces (Fawcett *et al*., 2019; Soles *et al*., 2023). Within this anatomical context, the reduced expression of *COL1A1* and *COL1A2* observed following chronic NaF exposure may indicate alteration in collagen-related ECM homeostasis. Such changes could potentially affect collagen-dependent structural support in collagen-rich compartments, particularly perivascular and meningeal regions, although the present study did not separately examine these anatomical compartments at the molecular level. This interpretation is consistent with the perivascular histopathological changes evident in our study.

These findings are consistent with previous studies that demonstrated significant fluoride induced disruption of type I collagen gene expression in skeletal muscles and dentin of rats (Gupta *et al*., 2014), in rat osteoblasts (Yan *et al*., 2011), and in dentin of guinea pig teeth (Han *et al.*, 2017). Our findings therefore support the previously recognized effects of fluoride on collagen metabolism in both mineralized and connective tissues, including the CNS, indicating that altered ECM synthesis and structural maintenance may contribute to fluoride-induced neural injury.

Our finding of reduced *MMP9* expression diverges from several previous reports and warrants careful consideration rather than selective citation. Qing-Feng *et al*., (2019) found that chronic fluorosis increased *MMP9* and *p53* expression in rats, with associated blood-brain barrier damage and neuronal apoptosis. Similarly, Łukomska *et al*., (2021) and Ai *et al*., (2025) reported altered *MMP2* and *MMP9* expression and related ECM-remodeling pathways upon fluoride exposure. This apparent discrepancy may reflect differences among studies in fluoride dose, exposure duration (experimental design), developmental stage, brain region examined. Importantly, reduced *MMP9* expression may reflect impaired ECM turnover and remodeling rather than a protective response.

Oxidative and inflammatory stress may provide a mechanistic link between chronic fluoride exposure and altered collagen expression. Previous studies have indicated that chronic fluoride exposure has been associated with reduced antioxidant capacity and activation of apoptotic pathways in the rat brain (Dahiru *et al.*, 2026) and hippocampal impairment (Bittencourt *et al.*, 2023). ROS and inflammatory signaling, particularly through the NF-κB pathway, have been implicated in the suppression of *COL1A1* and *COL1A2* transcription (Rippe *et al*., 1999).Therefore, fluoride-induced oxidative and inflammatory stress may impair collagen synthesis and MMP9-mediated remodeling, contributing to disrupted ECM homeostasis and alterations in the brain's structural microenvironment, consistent with the neuronal shrinkage and pyknosis observed in the present study.

Additionally, the apoptotic loss of matrix-producing cells documented in our earlier work together with the neuronal shrinkage and pyknosis (Dahiru *et al.* 2026), may further impair ECM synthesis and remodeling. Although the dose*sex interaction did not reach statistical significance, males showed a graded, monotonic decline in *COL1A1* and *COL1A2*, which may potentially reflect difference in the hormonal regulation of collagen expression between sexes. Markiewicz *et al*., (2013) demonstrated that both ERα and ERβ influence collagen biosynthesis in mouse skin, with receptor-specific and opposing effects on basal *Col1a1* transcript levels.

Because the normal rodent brain contains small amounts of fibrillar collagen outside the meninges and perivascular spaces (Soles *et al.*, 2023), the absence of blue trichrome staining in the control, low-, and medium-dose groups represents the expected histological appearance rather than a pathological finding. In contrast, the high-dose (300 ppm) group exhibited mild, blue-stained perivascular and interstitial collagen fibers, indicating a subtle increase in collagen deposition compared with normal brain tissue. Alongside these changes, progressive neuronal degeneration, extracellular edema, and disruption of the normal tissue architecture became more pronounced with increasing NaF exposure. These observations indicate that fluoride-associated neurotoxic effects are characterized primarily by neuronal injury, and structural disorganization, along with ECM alterations. A limitation of the present study is that individual water consumption was not measured daily. Thus, our estimated daily NaF exposure was based on an assumed water intake value (150 mL/Kg/day). Consequently, actual NaF intake may have varied among treatment groups and between sexes.

Our results support a potential mechanistic model in which fluoride-induced ROS production may contribute to altered extracellular matrix expression, with observed histopathological alterations serving as morphological endpoint of this molecular interplay.

Conclusion: Chronic fluoride exposure in rats for 90 days significantly altered extracellular matrix (ECM) homeostasis in the brain, as evidenced by the downregulation of matrix related genes *COL1A1, COL1A2* and *MMP9*. This coordinated reduction may indicate altered collagen synthesis and extracellular matrix remodeling, suggesting a disturbance in normal matrix turnover rather than a compensatory response. Such alterations in ECM dynamics may affect neuronal and perivascular integrity, potentially influencing processes involved in blood-brain barrier maintenance, neuroplasticity, and tissue repair, although these effects were not directly assessed in the present study. These findings provide further evidence that ECM dysregulation may contribute to fluoride-associated neural injury. Finally, the results highlight the potential vulnerability of brain extracellular matrix architecture to chronic fluoride exposure and support further investigation of matrix related molecular targets of long-term fluoride intake.

Competing Interest: We declare no conflict of interest, financial or personal, that could have influenced the report on this work.

Funding Sources: The work was supported by Pakistan High Education Commission (HEC) (Grant number: NRPU/HEC-14825-2021) and supported by Comsats University Islamabad (CUI).

Acknowledgement: We acknowledge the support of Comsats University Islamabad (CUI) scholarship, High Education Commission (HEC) Pakistan, National Institute of Health Pakistan (NIH), Shaheed Zulfiqar Ali Bhutto Medical University, Pakistan Institute of Medical Sciences and everyone who have helped us during this study.

REFERENCES

Aboghazleh, R., S. D. Boyajian, A. Atiyat, M. Udwan, M. Al-Helalat. and R. Al-Rashaideh (2024). Rodent brain extraction and dissection: A comprehensive approach. MethodsX. 12: 102516. https://doi.org/ 10.1016/ j.mex.2023.102516.

Ai, F., S. Wang, L. Ye, W. Wan, X. Zhou, M. Liu, M. Mo, Y. Lu, N. Wei, Z. Guan. and Y. Liu (2025). Chondroitin sulfate protects against synaptic impairment caused by fluorosis through the Erk1/2-MMP-9 signaling pathway. Sci. Rep. 15(1): 29760. https://doi.org/10.1038/s41598-025-14631-7.

Albus, U. (2012). Guide for the Care and Use of Laboratory Animals (8th edn). *Lab. Anim.* 46(3). https://doi.org/10.1258/la.2012.150312.

Bibi, S., R. Habib, S. Shafiq, S. S. Abbas, S. Khan, S. A. M. A. S. Eqani, E. Nepovimova, M. S. Khan, K. Kuca. and S. M. Nurulain (2023). Influence of the chronic groundwater fluoride consumption on cholinergic enzymes, ACHE and BCHE gene SNPs and pro-inflammatory cytokines: A study with Pakistani population groups. Sci. Total Environ. 1:880: 163359. https://doi.org/10.1016/j.scitotenv.2023.163359.

Bittencourt, L. O., A. Dionizio, M. K. M. Ferreira, W. A. B. Aragão, C. S. de Carvalho, B. Puty, F. M. C. do Socorro, F. V. Zohoori, M. A. R. Buzalaf. and R. R. Lima (2023). Prolonged exposure to high fluoride levels during adolescence to adulthood elicits molecular, morphological, and functional impairments in the hippocampus. Sci. Rep. 13(1): 11083. https://doi.org/10.1038/s41598-023-38096-8.

Chambers, A. F. and L. M. Matrisian (1997). Changing views of the role of matrix metalloproteinases in metastasis. J. Nalt. Cancer Inst. 89(17): 1260-1270. https://doi.org/10.1093/jnci/89.17.1260.

Cui, N., M. Hu. and R. A. Khalil (2017). Biochemical and Biological Attributes of Matrix Metalloproteinases. Prog. Mol. Biol. Transl. Sci. 147: 1-73. https://doi.org/10.1016/bs.pmbts.2017.02.005.

Dahiru, A., I. Nawaz, S. K. Riaz, S. S. Chaudry, M. J. Khan, Q. Huang, M. Abbas. and S. A. M. A. S. Eqani (2026). Molecular mechanisms underlaying fluoride-induced neurotoxicity: interplay of antioxidants and endoplasmic reticulum stress-mediated apoptotic pathways in rats. Naunyn Schmiedebergs Arch. Pharmacol. 399: 17291-17302. https://doi.org/10.1007/s00210-026-05441-3.

Fawcett, J. W., T. Oohashi. and T. Pizzorusso (2019). The roles of perineuronal nets and the perinodal extracellular matrix in neuronal function. Nat. Rev. Neurosci. 20: 451-465. https://doi.org/10.1038/s41583-019-0196-3.

Gupta, A. R., S. Dey, M. Saini. and D. Swarup (2014). Down-regulation of expression of type 1 collagen gene in dentin of fluoride exposed rats. Indian J. Anim. Res. 48(6): 601-604. https://doi.org/10.5958/0976-0555.2014.00039.9.

Han, T., M. Wang, C. Cao, H. Chen, G. Zhang, L. Wang. and J. Wang (2017). Fluoride or/and aluminum induced toxicity in guinea pig teeth with the low expression of dentine phosphoprotein. J. Biochem. Mol. Toxicol. 31(8): e21912. https://doi.org/10.1002/jbt.21912

Heindel, J. J., H. K. Bates, C. J. Price, M. C. Marr, C. B. Myers. and B. A. Schwetz (1996). Developmental toxicity evaluation of sodium fluoride administered to rats and rabbits in drinking water. Fundam. Appl. Toxicol. 30(2): 162-77. https://doi.org/10.1006/faat.1996.0053.

Jagtap, S., M. K. Yenkie, N. Labhsetwar. and S. Rayalu (2012). Fluoride in drinking water and defluoridation of water. Chem. Rev. 112(4): 2454-2466. https://doi.org/10.1021/cr2002855.

Johnston, N. R. and S. A. Strobel (2020). Principles of fluoride toxicity and the cellular response: a review. Arch. Toxicol. 94(4): 1051-1069. https://doi.org/10.1007/s00204-020-02687-5.

Kashyap, S. J., R. Sankannavar. and G. M. Madhu (2021). Fluoride sources, toxicity and fluorosis management techniques - A brief review. J. Hazard. Mater. Lett. 2: 100033. https://doi.org/10.1016/j.hazl.2021.100033.

Lacson, C. F. Z., M. C. Lu. and Y. H. Huang (2021). Fluoride-containing water: A global perspective and a pursuit to sustainable water defluoridation management -An overview. J. Clean. Prod. 280(1): 124236. https://doi.org/10.1016/j.jclepro.2020.124236.

Laronha, H. and J. Caldeira (2020). Structure and function of human matrix metalloproteinases. Cells. 9(5): 1076. https://doi.org/10.3390/cells9051076.

Liu, J. and R. A. Khalil (2017). Matrix Metalloproteinase Inhibitors as Investigational and Therapeutic Tools in Unrestrained Tissue Remodeling and Pathological Disorders. Prog. Mol. Biol. Transl. Sci. 148: 355-420. https://doi.org/10.1016/bs.pmbts.2017.04.003.

Łukomska, A., I. Baranowska-Bosiacka, K. Dec, A. Pilutin, M. Tarnowski, K. Jakubczyk, W. Żwierełło, M. Skórka-Majewicz, D. Chlubek. and I. Gutowska (2021). Changes in gene and protein expression of metalloproteinase-2 and -9 and their inhibitors TIMP2 AND TIMP3 in different parts of fluoride-exposed rat Brain. Int. J. Mol. Sci. 22(1): 391. https://doi.org/10.3390/ijms22010391.

Malemud, C. J. (2006). Matrix metalloproteinases (MMPs) in health and disease: An overview. 11: 1696-701 *Front. Biosci*. https://doi.org/10.2741/1915.

Markiewicz, M., S. Znoyko, L. Stawski, A. Ghatnekar, G. Gilkeson. and M. Trojanowska (2013). A role for estrogen receptor-α and estrogen receptor-β in collagen biosynthesis in mouse skin. J. Invest. Dermatol. 133(1): 120-7. https://doi.org/10.1038/jid.2012.264.

Mullenix, P. J., P. K. Denbesten, A. Schunior. and W. J. Kernan (1995). Neurotoxicity of sodium fluoride in rats. Neurotoxicol. Teratol. 17(2): 169-77. https://doi.org/10.1016/0892-0362(94)00070-T.

Myllyharju, J. and K. I. Kivirikko (2004). Collagens, modifying enzymes and their mutations in humans, flies and worms. Trends Genet. 20(1): 33-43. https://doi.org/10.1016/j.tig.2003.11.004.

Qing-Feng, S., X. Tian-Tong. and X. Ying-Peng (2019). Matrix metalloproteinase-9 and p53 involved in chronic fluorosis induced blood-brain barrier damage and neurocyte changes. Arch. Med. Sci. 15(2): 457-466. https://doi.org/10.5114/aoms.2019.83294.

Ren, C., H. H. Li, C. Y. Zhang. and X. C. Song (2022). Effects of chronic fluorosis on the brain. Ecotoxicol. Environ. Saf. 244: 114021. https://doi.org/10.1016/j.ecoenv.2022.114021.

Rippe, R. A., L. W. Schrum, B. Stefanovic, J. A. Solís-Herruzo. and D. A. Brenner (1999). NF-κB inhibits expression of the α1(I) collagen gene. DNA Cell Biol. 18(10): 751-61. https://doi.org/10.1089/104454999314890.

Rutnam, Z. J., T. N. Wight. and B. B. Yang (2013). miRNAs regulate expression and function of extracellular matrix molecules. Matrix Biol. 32(2): 74-85. https://doi.org/10.1016/j.matbio.2012.11.003.

Sadiq, M., S. A. M. A. S. Eqani, I. Nawaz, N. Bangash, S. Ilyas, J. Podgorski. and M. Berg (2025). Fluoride contamination of groundwater in different geological settings of Punjab Province, Pakistan: Levels, possible mechanisms and health risks. Sci. Total Environ. 1001: 180450. https://doi.org/10.1016/j.scitotenv.2025.180450.

Sharma, U., L. Carrique, S. Vadon-Le Goff, N. Mariano, R. N. Georges, F. Delolme, P. Koivunen, J. Myllyharju, C. Moali, N. Aghajari. and D. J. S. Hulmes (2017). Structural basis of homo- and heterotrimerization of collagen I. Nat. Commun. 8: 14671. https://doi.org/10.1038/ncomms14671

Soles, A., A. Selimovic, K. Sbrocco, F. Ghannoum, K. Hamel, E. L. Moncada, S. Gilliat. and M. Cvetanovic (2023). Extracellular Matrix Regulation in Physiology and in Brain Disease. Int. J. Mol. Sci. 24(8): 7049. https://doi.org/10.3390/ijms24087049.

Tonetto, S., P. Weikop, T. Brudek. and M. Thomsen (2023). Behavioral and biochemical effects of alcohol withdrawal in female C3H/HeNRj and C57BL/6JRj mice. Front. in Behav. Neurosci. 17:1143720. https://doi.org/10.3389/fnbeh.2023.1143720.

Varner, J. A., K. F. Jensen, W. Horvath. and R. L. Isaacson (1998). Chronic administration of aluminum-fluoride or sodium-fluoride to rats in drinking water: Alterations in neuronal and cerebrovascular integrity. Brain Res. 784(1-2): 284-98. https://doi.org/10.1016/S0006-8993(97)01336-X.

Yan, X., X. Yan, A. Morrison, T. Han, Q. Chen, J. Li. and J. Wang (2011). Fluoride induces apoptosis and alters collagen I expression in rat osteoblasts. Toxico. Lett. 200(3): 133-8. https://doi.org/10.1016/j.toxlet.2010.11.005.

Zhu, J., C. L. Hoop, D. A. Case. and J. Baum (2018). Cryptic binding sites become accessible through surface reconstruction of the type I collagen fibril. Sci. Rep. 8(1): 16646. https://doi.org/10.1038/s41598-018-34616-z.